

# On the identification and characterization of outdoor thermo-hygrometric stress events

Serena Falasca<sup>a,\*</sup>, Annalisa Di Bernardino<sup>a</sup>, Ferdinando Salata<sup>b</sup>

<sup>a</sup> Department of Physics, "Sapienza" University of Rome, Piazzale Aldo Moro 5, 00185 Rome, Italy

<sup>b</sup> Department of Astronautical, Electrical and Energy Engineering (DIAEE), "Sapienza" University of Rome, Via Eudossiana 18, 00184 Rome, Italy

## ARTICLE INFO

### Keywords:

MOCI  
Urban heat island  
Heat wave indices  
Extreme temperatures  
Thermal stress  
Po valley

## ABSTRACT

Human thermal sensations are not controlled merely by the ambient temperature, but also by other biometeorological variables and personal factors. Therefore, thermo-hygrometric stress events need to be identified and monitored in addition to heat waves. The purpose of the present article is proposing a method for detection and characterization of thermo-hygrometric stress events, based on the rearrangement of heat waves indices and on new quantities. The Mediterranean Outdoor Thermal Comfort Index (MOCI) is used as a reference variable instead of the air temperature. The method is applied to Milan (Italy) for the 2022 summer, which: i) is the hottest in the period 1991–2020 with a temperature anomaly of 3.17 °C and ii) presents higher minimum temperatures (1.5 times higher) than those of the control period. The analysis of daytime values of MOCI demonstrates a cumulative MOCI higher than zero only in 2022. Hence, the lower fraction of data in the cold range determines a significant increase in the cumulative MOCI. The metrics on severe MOCI events in 2022 confirm the key-role of extreme temperatures. The proposed method is effective and, in this case, reveals the relevance of the cumulative thermal and thermo-hygrometric loads also in the absence of critical heating conditions.

## 1. Introduction

There is nowadays generalized evidence of a progressive increase in the global surface temperature. A recent (dated May 9th, 2022) WMO update estimated "a 50:50 chance of the annual average global temperature temporarily reaching 1.5 °C above the pre-industrial level for at least one year between 2022–2026", which is the lower target of the Paris Agreement on Climate Change (WMO, 2022). In Europe, annual temperature has increased at an average rate of 0.15 °C per decade since 1910 and of 0.45 °C since 1981. Furthermore, the ten warmest years were recorded since 2007 (NOAA, 2022).

In addition to the official reports of national and international institutions (e.g., Intergovernmental Panel on Climate Change, US National Oceanic and Atmospheric Administration, European Environment Agency), also a plenty of recent scientific publications have been focused on observed and projected trends of temperature and precipitation (e.g., Viceto et al., 2019; Fanta et al., 2022; Lomakina and Lavrinenko, 2022), heat waves (HWs) (Fischer and Schär, 2010; Mbokodo et al., 2020; Perkins-Kirkpatrick and Lewis, 2020) and other extreme weather events (e.g., Tang, 2019; Almazroui, 2020). Great emphasis is still placed on different aspects of HWs, that can be broadly considered as "a period of consecutive days where conditions are excessively hotter than normal" (Perkins and Alexander,

\* Corresponding author.

E-mail addresses: [serena.falasca@uniroma1.it](mailto:serena.falasca@uniroma1.it) (S. Falasca), [annalisa.dibernardino@uniroma1.it](mailto:annalisa.dibernardino@uniroma1.it) (A. Di Bernardino), [ferdinando.salata@uniroma1.it](mailto:ferdinando.salata@uniroma1.it) (F. Salata).

<https://doi.org/10.1016/j.uclim.2023.101728>

Received 14 November 2022; Received in revised form 26 April 2023; Accepted 22 October 2023

Available online 27 October 2023

2212-0955/© 2023 The Authors. Published by Elsevier B.V. This is an open access article under the CC BY license (<http://creativecommons.org/licenses/by/4.0/>).

2013a) or “from the human health point of view, a heat (cold) wave can be considered as a period with sustained temperature anomalies resulting in one of a number of health outcomes, including mortality, morbidity and emergency service callout” (Kovats and Kristie, 2006; Lavaysse et al., 2018). Moreover, since findings largely agree on a progressive intensification of these severe events, multiple metrics (based on different criteria) have been developed to quantitatively describe and compare HWs occurring in different geographical areas on the globe (Perkins and Alexander, 2013b).

### 1.1. Literature review

Several studies underline that the Mediterranean region is heavily affected by global warming with a significant alteration in extreme temperatures and HWs intensity, frequency, and duration. Perkins-Kirkpatrick and Gibson (2017) estimated the variation of HWs characteristics with respect to climate change thresholds on the basis of the two global climate model ensembles Coupled Model Intercomparison Project (CMIP5) and Community Earth System Model (CESM) and showed that the Mediterranean and Eurasian areas will experience the largest increase in HW intensity with peaks even higher than 8 °C by 2100 without constraints to the global warming. Such results confirmed the projections by King and Karoly (2017) who focused on the global warming thresholds of 1.5 °C and 2 °C. According to Zittis et al. (2016), the Mediterranean region could experience in the future HWs with amplitudes increased by 6–10 °C. Lionello and Scarascia (2018) also analyzed modelled datasets founding that in the twenty-first century in the Mediterranean region temperatures will increase 20% more than the global average. Also for the Italian peninsula, located in the middle of the Mediterranean basin, a general warming trend in terms of temperature and daily extremes in the last decades has been confirmed. Scorzini and Leopardi (2019) performed a climatological study for a region of Central Italy, showing a mean annual temperature trend of +0.15 °C/decade over the last 60 years, even more relevant in the spring and summer. Di Bernardino et al. (2022) also conducted a trend study over a period of two decades for the city of Rome and surroundings, founding an increase of 0.07 °C/year in urban and coastal sites for the average temperature and of 0.10 °C/year and 0.01 °C/year for maximum and minimum temperatures in the urban and coastal environments, respectively. In Northern Italy, the Po basin, due to its peculiar morphology, presents weather conditions associated with low diffusive properties of the atmosphere, such as calm wind conditions, limited extension of the planetary boundary layer, and temperature inversions (Caserini et al., 2017). The Po valley is recognized as a hotspot for pollution in Europe also due to the high concentration of anthropogenic sources as shown by Ferrero et al. (2019) thanks to the application of a new developed hybrid algorithm able to detect concentrations of particulate matter from satellite aerosol optical depth data. Besides, research suggests that conditions of poor air quality can be concomitant with thermo-hygrometric discomfort, aggravating health risks of people. Both Khomsi et al. (2022) and Falasca et al. (2021) focused on the concurrence of thermal and thermo-hygrometric stress conditions and extreme surface ozone events due to the photochemical nature of surface ozone. Moreover, Falasca et al. (2021) suggested to use thermo-hygrometric stress conditions as an alert and detection tool for severe surface ozone episodes.

The increase in temperatures linked to climate change adds up in urban areas to the typical overheating known as urban heat island (UHI). The combination of the two phenomena affects the life quality of city inhabitants from multiple points of view, such as energy consumption (Wang et al., 2023) and outdoor thermo-hygrometric comfort (OTC). Regarding the first topic, Li et al. (2019) have quantified the average impact of the UHI on energy consumption for cooling and heating of buildings equal to +19.0% and –18.7%, respectively. The large intercity differences cause a range from 10% to 120% for cooling and from 3% to 45% for heating, and intra-city differences were also noted (Li et al., 2019). Concerning the OTC, the association between thermal sensations and urbanization degree within the same city has been highlighted in several studies focused in different geographical areas. For example, Balogun and Dar-amola (2019) explored the impact of the urban fabric on the human thermal sensations in Nigeria in terms of the Temperature Humidity Index thanks to a field measurement campaign conducted during the entire year of 2009. Falasca et al. (2022) performed a similar study for the city of Rome (Italy) investigating the variability of the Mediterranean Outdoor Comfort Index (MOCI) with the local environmental conditions using observations acquired at urban, suburban, rural sites (Falasca et al., 2022). Shooshtarian et al. (2020) provided a review of the scientific articles on the outdoor thermal comfort in Australian cities recognizing the urbanization as a major factor in elevated daily temperatures in Australia. They also indicated the topics not covered in the existing literature and the approaches and aspects that should be considered in the future works (Shooshtarian et al., 2020). Similarly, in their review Lai et al. (2019) stated that the two main challenges facing the urban outdoor thermal environment are global warming and UHIs.

Several studies investigated the climate-change related evolution of OTC. For example, Tomczyk et al. (2020) investigated the human-biometeorological conditions during heat waves in Poland in the period 1966–2018 using the Physiologically Equivalent Temperature (PET) as biometeorological index. Some studies employed observations for the calculation of the biometeorological indices as Rozbicka and Rozbicki (2021) did with the Universal Thermal Comfort Index (UTCI) still in Poland. Others used other gridded datasets (e.g., as ERA-Interim reanalysis) that allow both spatial and temporal characterization of PET and UTCI, such as Varentsov et al. (2020) in Russia and Zeng et al. (2020) in China. Moreover, the recent research carried out by Shin et al. (2022) on air temperature and OTC (i.e., thermal comfort indices) trends in South Korea revealed a larger thermal health risk than the one expected on the basis of the annual mean temperature (Shin et al., 2022).

Air temperature is the main driver of the OTC, nevertheless other biometeorological (or bioclimatic) parameters together with personal conditions (e.g., humidity, wind speed, clothing, health state) contribute to the individual thermal sensations. Most of the previous studies examined OTC conditions during extreme high temperatures (e.g., Bajšanski et al., 2015; Unger et al., 2020) while the monitoring or search of outdoor thermal stress episodes through bioclimatic metrics is unusual.

## 1.2. Aims and novelty of the work

This research aims at filling the scientific gap described in Section 1.1 by arranging a new framework for the identification and evaluation of the thermo-hygro-metric stress events based on: i) rearranged indices developed for HWS, ii) new indices specifically designed. To this end, OTC conditions occurred during the exceptionally hot summer of 2022 ([https://www.isac.cnr.it/climstor/climate\\_news.html](https://www.isac.cnr.it/climstor/climate_news.html), last accessed on 11st October 2022) in Milan (Po valley) are investigated.

The Mediterranean Outdoor Comfort Index (MOCI) (Salata et al., 2016) is adopted as reference parameter among the existing metrics since this work focuses on an Italian city belonging to the Mediterranean region. Parameters incorporating both minimum and maximum temperatures and the overall thermal load to which the human body is exposed are required, such as cumulative temperature and MOCI are also required given that the trend towards longer and hotter summers associated to the climate change in the Mediterranean area (Cramer et al., 2018; Linares et al., 2020) can affect people's sensitivity to air temperature.

## 2. Methodology

### 2.1. Site description

Milan is one of the major cities in northern Italy and one of the most populous areas in Europe, hosting about 1.4 million inhabitants (ISTAT, 2022).

Milan is located in the western region of the Po valley (Fig. 1, left panel), which extends from the Western Alps to the Adriatic Sea, and which is widely recognized as a hotspot for atmospheric pollution (Putaud et al., 2010). According to the Köppen-Geiger climate classification (Beck et al., 2018), Milan belongs to the Cfa class, i.e., it is characterized by a humid temperate climate with a significant annual temperature excursion. The data used in this study are provided by the local regional environmental protection agency (ARPA Lombardia) network. Among all the stations managed by ARPA Lombardia, only two stations in downtown Milan provide all the weather variables required in this work (i.e., dry-bulb temperature, relative humidity, wind velocity, global solar radiation). Among them, the Juvara station (Lat. 45.47 N, Lon. 9.22 E, 122 m a.s.l.) is the one providing the longest time series and has therefore been selected for the present study as representative of the micrometeorological conditions of Milan, being in a highly urbanized portion of the city center (Fig. 1, right panel). Table 1 summarizes the technical characteristics of the sensors.

### 2.2. The Mediterranean Outdoor Thermal Comfort Index (MOCI)

The Mediterranean Outdoor Thermal Comfort Index (MOCI) is a thermo-hygro-metric comfort index for outdoor environments developed to precisely associate a numerical quantity to thermal sensations expressed by a statistically valid sample of residents in the Mediterranean region and therefore adapted to the local climate (Salata et al., 2016). Compared to previous indexes based on the sensations experienced by samples of residents in Northern Europe and Northern America, the MOCI can better reproduce the thermal sensations expressed by the Mediterranean normotype. This feature of the MOCI compared to other indices has been investigated in (Golasi et al., 2016) where the advantages of its application are demonstrated.

MOCI is based on an ASHRAE 7-point scale and allows quantification of the thermal sensations of a Mediterranean normotype. It has been obtained thanks to a robust statistical survey and a subsequent Subsets Analysis. Compared to other previously proposed indices (e.g., the Active Sensation Vote Europe, the Effective Temperature, the Physiological Equivalent Temperature, and the Predicted Mean Vote), MOCI turned out to be more effective in predicting individual thermal sensations (Golasi et al., 2016).

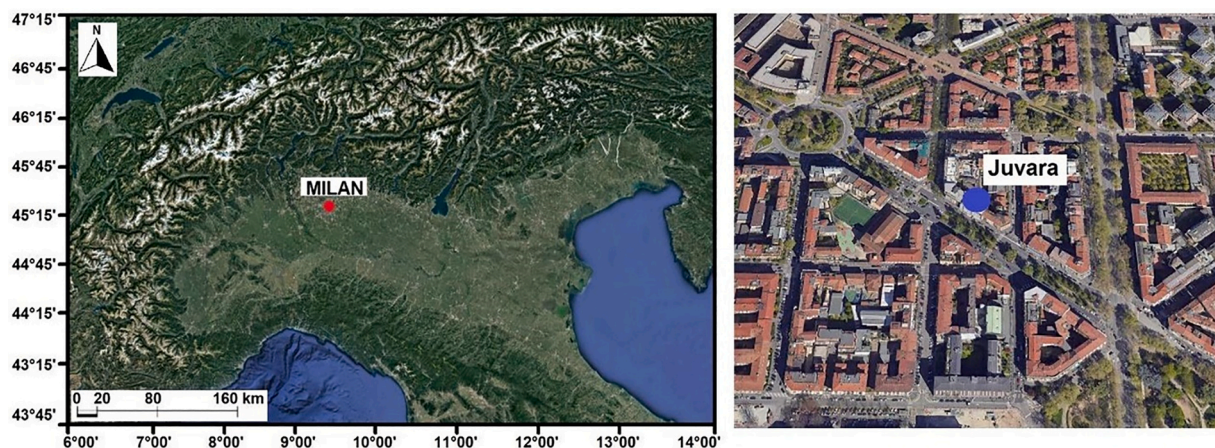


Fig. 1. Geographical map of northern Italy, the red dot identified the city of Milan (left panel). Enlargement of the urban fabric adjacent to the Juvara station (blue dot, right panel). (For interpretation of the references to colour in this figure legend, the reader is referred to the web version of this article.)

**Table 1**  
Technical characteristics of the sensors installed at the Juvara station.

| Variable               | Sensor           | Accuracy   | Range                         | Resolution             |
|------------------------|------------------|--|-------------------------------|------------------------|
| Dry-bulb temperature   | Thermohygrometer | $\pm 0.10$ °C  | $-50 \div 70$ °C              | 0.06 °C                |
| Relative humidity      | Thermohygrometer | $\pm 1.5\%$  | $0 \div 100\%$                | 0.50%                  |
| Wind velocity          | Tachoaemometer   | $< 35 \text{ ms}^{-1}$ : $\pm 2\%$<br>$> 35 \text{ ms}^{-1}$ : $\pm 3\%$ | $0 \div 50 \text{ ms}^{-1}$   | $0,01 \text{ ms}^{-1}$ |
| Wind direction         | Gonioaemometer   | $\pm 2^\circ$  | $0 \div 360^\circ$            | $1^\circ$              |
| Global solar radiation | Pyranometer      | $\pm 5\%$  | $0 \div 1500 \text{ Wm}^{-2}$ | $1 \text{ Wm}^{-2}$    |

It is defined as follows Eq. (1):

$$MOCI = -4.257 + 0.146 \bullet T_A + 0.325 \bullet I_{CL} + 0.005 \bullet RH + 0.001 \bullet I_S - 0.235 \bullet W_S \quad (1)$$

where:

- $T_A$  is the air temperature [°C]
- $I_{CL}$  is the thermal resistance of the clothing, defined as a function of the air temperature (Eq. (2)):

$$I_{CL} = 1.608 - 0.038 \bullet T_A \quad (2)$$

- RH is the relative humidity [%]
- $I_S$  is the solar radiation [ $\text{Wm}^{-2}$ ]
- $W_S$  is the wind speed [ $\text{ms}^{-1}$ ].

MOCI values are computed in Milan at the location corresponding to the Juvara station of the ARPA Lombardia network by inserting in Eq. (1) weather quantities (i.e., air temperature, relative humidity, solar radiation and wind speed) measured hourly by the Juvara station itself (Section 2.1). Similarly to other indices based on a 7-point scale, thermal comfort conditions correspond to MOCI values in the range between  $-0.5$  and  $0.5$ . Values higher than  $0.5$  imply a sensation of increasing heat in the Mediterranean normotype, while values lower than  $-0.5$  imply a sensation of increasing cold. Although the MOCI has been developed for people acclimatized to the Mediterranean climate (“Cs- Csa” according to the Koppen-Geiger classification), previous applications have also shown its validity in the city of Milan (Falasca et al., 2019; Falasca et al., 2021).

### 2.3. Data collection and processing

In this work, two different datasets of weather variables have been employed, both based on acquisitions from the Juvara station of ARPA Lombardia for the May–August season (Section 2.1).

In more detail:

1. Hourly air temperature time series recorded from 1990 to 2022 (download at the web page <https://www.arpalombardia.it/Pages/Meteorologia/Richiesta-dati-misurati.aspx>, in Italian, last accessed on 31st October 2022). The years of 2007 and 2012 have been excluded due to an amount of missing data higher than 25%;
2. Hourly air temperature, wind speed intensity, global radiation, relative humidity (required to compute MOCI) time series acquired from 2014 to 2022 (download at the web page <https://www.arpalombardia.it/Pages/Meteorologia/Richiesta-dati-misurati.aspx>, in Italian, last accessed on 31st October 2022). This time span has been chosen based on the availability of the four variables. This dataset has been processed in order to standardize the data available in each year of the timespan: i) for each missing data in a certain time step of a year (for example, June 5th, 2014 at 08:00) the data corresponding to the same time step (June 5th at 08:00) in all the other years of the period have been removed; ii) only daytime data ranging from 8:00 to 22:00 CET have been examined. The MOCI dataset derived from these weather quantities is analyzed through the parameters described in Section 2.4.2.

### 2.4. Indices for the characterization of extremes in temperature and thermo-hygrometric sensations

This Section presents and describes the climate science indices selected for this work among those conceived for the characterization of temperature events. Some indices (see Section 2.4.1), are applied here to analyze the year 2022 with respect to the thirty-year period 1991–2020. Other indices (see Section 2.4.2), specifically defined for the HWs, are implemented for thermo-hygrometric stress events in the time span 2014–2022 adopting MOCI instead of temperature as the reference variable.

#### 2.4.1. Hot days, tropical nights, combined hot days and tropical nights and intraannual extreme temperature range

In this work, the following metrics are considered:

- Hot Days (HD): summer days with maximum temperatures exceeding  $35$  °C (Fischer and Schär, 2010)

- Tropical Nights (TN): summer days with minimum temperatures exceeding 20 °C (Fischer and Schär, 2010)
- Combined Hot days and Tropical nights (CHT): number of summer days with maximum temperatures exceeding 35 °C and minimum temperatures exceeding 20 °C (Fischer and Schär, 2010)
- Intraannual extreme temperature range (ETR): difference between the highest temperature observation for any given calendar year and the lowest temperature reading of the same calendar year (Russo and Sterl, 2011)

HD, TN and CHT depend on absolute temperature thresholds, and this could appear as a limitation in their applicability in different regions worldwide. However, they are commonly employed in areas with different climates (Chen and Lu, 2014; Graczyk et al., 2017; Khan et al., 2022) and Fischer and Schär (2010) demonstrated their robustness regardless of various factors (social, demographic, etc.).

2.4.2. Extreme temperature indices and their application to the outdoor thermo-hygrometric stress

In this work, the surveying of outdoor thermo-hygrometric stress events is based on the rearrangement of definitions and metrics typical of the climate science glossary. The climate science literature provides a wide range of indices for the detection of extreme temperature events (Perkins and Alexander, 2013a). More specifically, several definitions of the HW exist and the following is applied here: “a spell of at least six consecutive days with maximum temperatures exceeding the local 90th percentile of the control period” (Fischer and Schär, 2010). It is consistent with the definition of the warm spell duration index, that is the “annual count of days with at least six consecutive days when the daily maximum temperature is higher than the 90th percentile” (ETCCDI, 2020).

Borrowing from above, an “event” of outdoor thermo-hygrometric stress is defined as a period of at least six consecutive days characterized by maximum daily values of MOCI always above the comfort threshold (i.e., MOCI >0.5). Such a definition has been already applied in Falasca et al. (2021). For simplicity, outdoor thermo-hygrometric stress events are also referred to as “severe MOCI events” throughout the manuscript.

The following set of HW metrics used here is:

- HW frequency (HWF): sum of all HW days (Perkins-Kirkpatrick and Lewis, 2020);
- HW intensity (HWD): the average intensity across all HW days (Perkins-Kirkpatrick and Lewis, 2020);
- HW Duration (HWD): duration of the longest event (Perkins-Kirkpatrick and Lewis, 2020);
- Cumulative heat (CH, defined as in Eq. (3)): extra heat produced by HWs over a given season computed as the sum of the anomaly (Tanom) between each HW day (h in Eq. (3)) and the calendar-day 90th percentile across all HW days in that season (Perkins-Kirkpatrick and Lewis, 2020):

$$CH = \sum_{h=1}^n T_{anom} \tag{3}$$

The corresponding metrics related to thermo-hygrometric stress and derived from the above are:

- Thermo-hygrometric stress events frequency: sum of all MOCI events days
- Thermo-hygrometric stress events intensity: the average intensity across all MOCI events days
- Thermo-hygrometric stress events duration: duration of the longest MOCI event
- Cumulative extra-MOCI for thermo-hygrometric stress events days, defined as in Eq. (4):

$$Cumulative\ extra - MOCI = \sum_{h=1}^n (MOCImax - 0.5) \tag{4}$$

where *n* is the total number of days of severe MOCI and *h* the corresponding index, *MOCImax* is the maximum MOCI on day *h* and 0.5 is

**Table 2**  
Summary of derived and new indices for the characterization of outdoor thermo-hygrometric stress events.

| Type                            | Index                           | Definition for HWs  | Definition for outdoor thermo-hygrometric stress (severe MOCI) events  |
|---------------------------------|---------------------------------|---|--|
| Adapted from HWs                | Event                           | A spell of at least six consecutive days with maximum temperatures exceeding the local 90th percentile of the control period (Fischer and Schär, 2010)  | A period of at least six consecutive days characterized by maximum daily values of MOCI always above the comfort threshold (i.e., MOCI >0.5) |
| Adapted from HWs                | Frequency                       | Sum of all HW days (Perkins-Kirkpatrick and Lewis, 2020)  | Sum of all MOCI events days  |
| Adapted from HWs                | Intensity                       | Average intensity across all HW days (Perkins-Kirkpatrick and Lewis, 2020)  | Average intensity across all MOCI events days  |
| Adapted from HWs                | Duration                        | Duration of the longest event (Perkins-Kirkpatrick and Lewis, 2020)   | Duration of the longest event  |
| Adapted from HWs                | Cumulative heat and extra-MOCI  | Extra heat produced by HWs over a given season computed as the sum of the anomaly between each HW day and the calendar-day 90th percentile across all HW days in that season (Perkins-Kirkpatrick and Lewis, 2020). See Eq. (3) | Cumulative extra-MOCI for thermo-hygrometric stress events days. See Eq. (4)   |
| Introduced in the present study | Cumulative temperature and MOCI | Sum of hourly temperatures across the season  | Sum of hourly MOCI data across the season  |

the thermo-hygrometric comfort threshold.

The following quantities are also introduced and applied:

- Cumulative temperature: sum of hourly temperatures across the season
- Cumulative MOCI: sum of hourly MOCI data across the season

Table 2 provides a comparison of the indices described above, distinguishing between those developed in this work and those derived from existing ones.

### 3. Results

This Section presents the results of the analysis and is divided into two parts. The former Subsection focuses on the temperature characterization of the year 2022 with respect to the reference period 1991–2020 and is based on the application of temperature anomaly, minimum and maximum monthly temperatures, ETR, number of HD, TN and CHT (Section 2.4.1). This analysis permits to highlight the peculiar characteristics (in terms of temperature) of 2022 compared to the other years included in the dataset. The latter Subsection considers a more recent and limited dataset (i.e., 2014–2022) bound to the availability of all the quantities required for the calculation of the MOCI. It is based also on the application of the indices described in Section 2.4.2 and summarized in Table 3. This part is in turn divided into three Subsections focused on temperature, MOCI, and thermo-hygrometric stress (or severe MOCI) events, respectively.

#### 3.1. Analysis of the summer 2022 compared to the reference period 1991–2020

The May–September 2022 season is analyzed here with respect to the reference period 1991–2020 following the metrics introduced in Section 2.4.1, i.e.: i) temperature anomaly with respect to the average values of the control period (Fig. 2), ii) minimum and maximum monthly temperatures (Table 3), iii) ETR (Fig. 3), and iv) number of HD, TN and CHT (Fig. 4).

Fig. 2 shows the temperature anomaly of the years 1990–2022 compared to the average of the reference period 1991–2020 (equal to 22.9 °C). Seven of the twelve years with a positive anomaly (corresponding to about 39%) are in the last decade. More in detail, from 2015 onwards, only the year 2016 shows a negative anomaly, equal to  $-0.07$  °C. Among the years under investigation, the year 2022 experiences the highest temperature anomaly (equal to 3.17 °C), even higher than that of 2003 (equal to 2.63 °C), which is considered the hottest year of recent decades in Europe (García-Herrera et al., 2010). In addition to 2003 and 2022, the years 2015, 2017, 2018, and 2019 exhibit anomalies higher than 1 °C. The maximum absolute negative anomalies (equal to about 1.3 °C) have been recorded in 1995 and 1996.

The same type of analysis has been carried out for the individual months from May to August (Fig. 2b). May has a positive anomaly in more than half of the years of the control period. The year 2022 shows the highest anomaly (2.92 °C), although 2009 presents a very high value (2.5 °C), too. During June many positive anomalies are identifiable, with 2019, 2003 and 2022 experiencing the highest values (close to 4 °C). During July the years 2015 and 2022 have anomalies close to 4 °C and the 2003 an anomaly below 1 °C. In the year 2022, the August anomaly is the lowest between the months considered (equal to 2.07 °C) and the fifth highest in the control period, with 2003 again first in the ranking.

As for the minimum and maximum values of the temperature during the May–August season (Table 3), it is worth noting that the year 2022 has much higher minimum temperatures than those of the control period. The ratio between the minimum temperature in 2022 and that of the control period is higher than 1.5 in all the months considered and it even exceeds 2 during May. Contrariwise, monthly maximum temperatures in 2022 are lower than those of the control period, except for July, when they are comparable. Moreover, the maximum temperature difference between the year 2022 and the control period reaches 4 °C in June, while it is much less pronounced in the other months.

From the ETR point of view, the year 2022 (about 24.7 °C) does not present significant differences with respect to the control period. The highest ETR values refer to the years 2019 and 2017 ( $> 30$  °C), while the years 1999 and 1990 show the lowest values ( $< 20$  °C).

HD, TN and CHT have been also computed for the period 1990–2022 (Fig. 4). Our results show a higher number of TNs compared to HDs, the latter representing very low percentages in most years and being absent in the 90s and 2000s, apart from 2003 (5% of HD), 2006 (1.6% of HD), and 1998 (0.9% of HD). Since 2010 the percentage of HD increases approaching 10% in 2019 (9.6% of HD) and 2022 (7.3% of HD). On the other hand, the percentages of TN are frequently close to (and even higher than) 40% and reaches the

**Table 3**

Minimum and maximum temperatures for single months in the control period 1991–2020 and in the year of 2022.

| Month  | Minimum temperature [°C] |      | Maximum temperature [°C] |      |
|--------|--------------------------|------|--------------------------|------|
|        | 1990–2021                | 2022 | 1990–2021                | 2022 |
| May    | 5.4                      | 12.6 | 32.6                     | 31.9 |
| June   | 9.9                      | 18   | 38.5                     | 34.6 |
| July   | 13.1                     | 20.6 | 37.1                     | 37.3 |
| August | 11.8                     | 19.3 | 37.8                     | 36.5 |

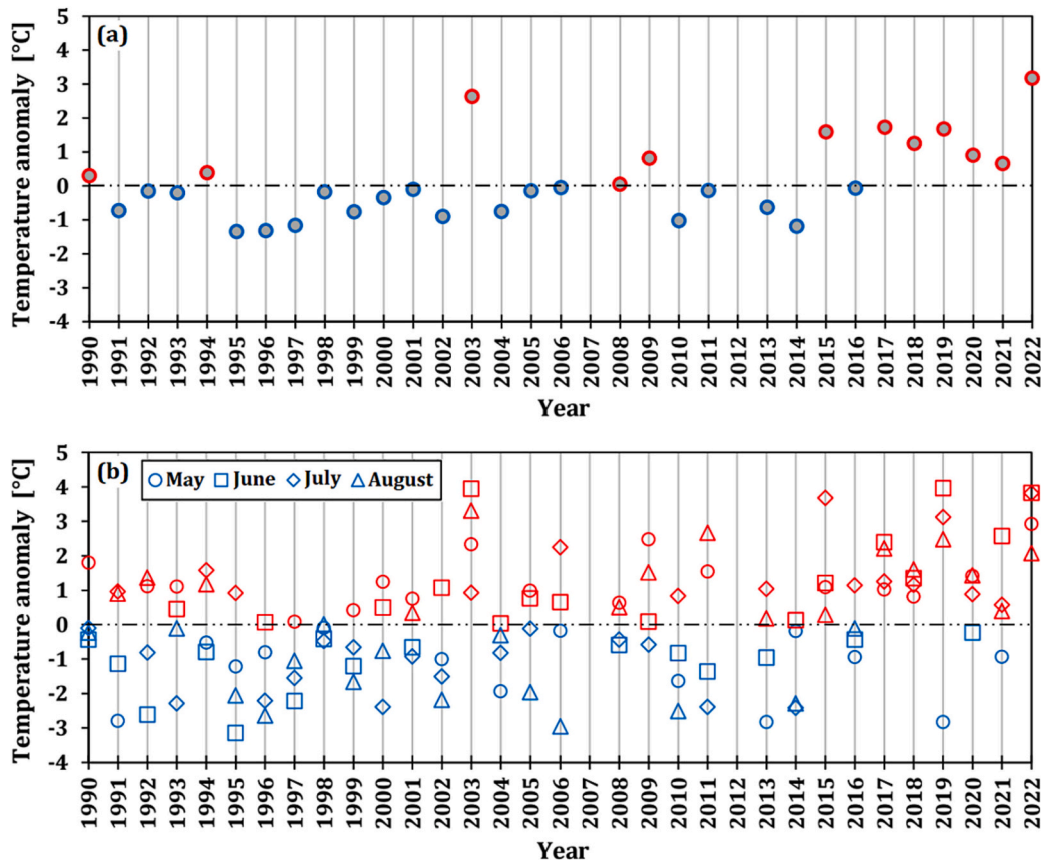


Fig. 2. Temperature anomaly with respect to the control period 1991–2020 for: a) annual mean, b) monthly mean. Blue denotes negative anomalies and red denotes positive anomalies.

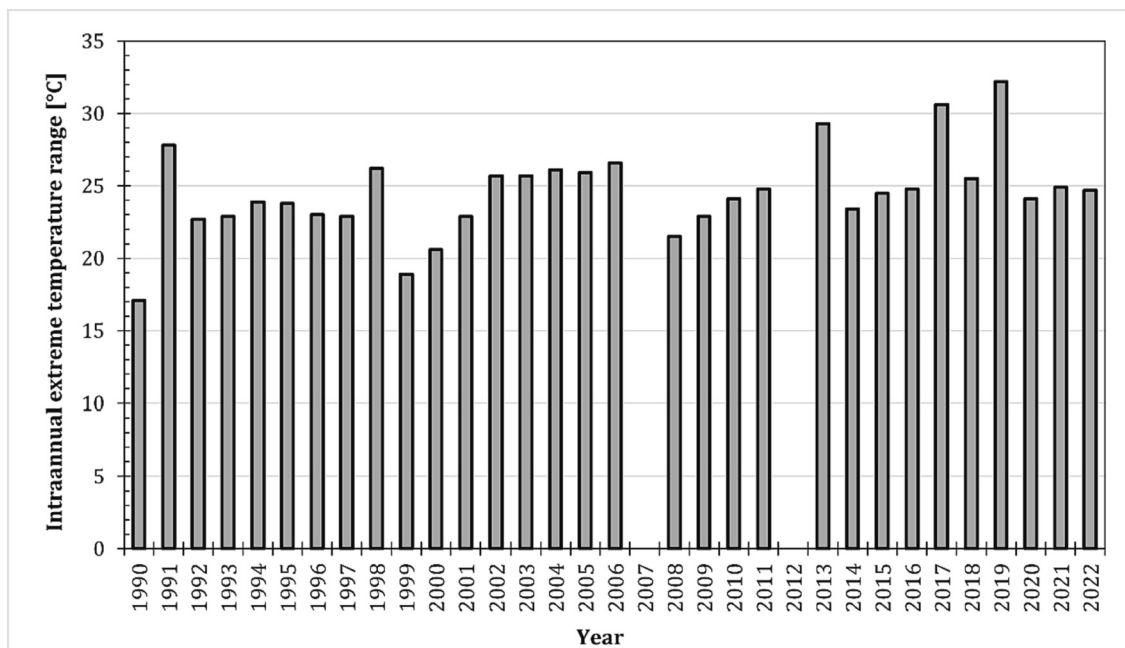


Fig. 3. Interannual extreme temperature range.

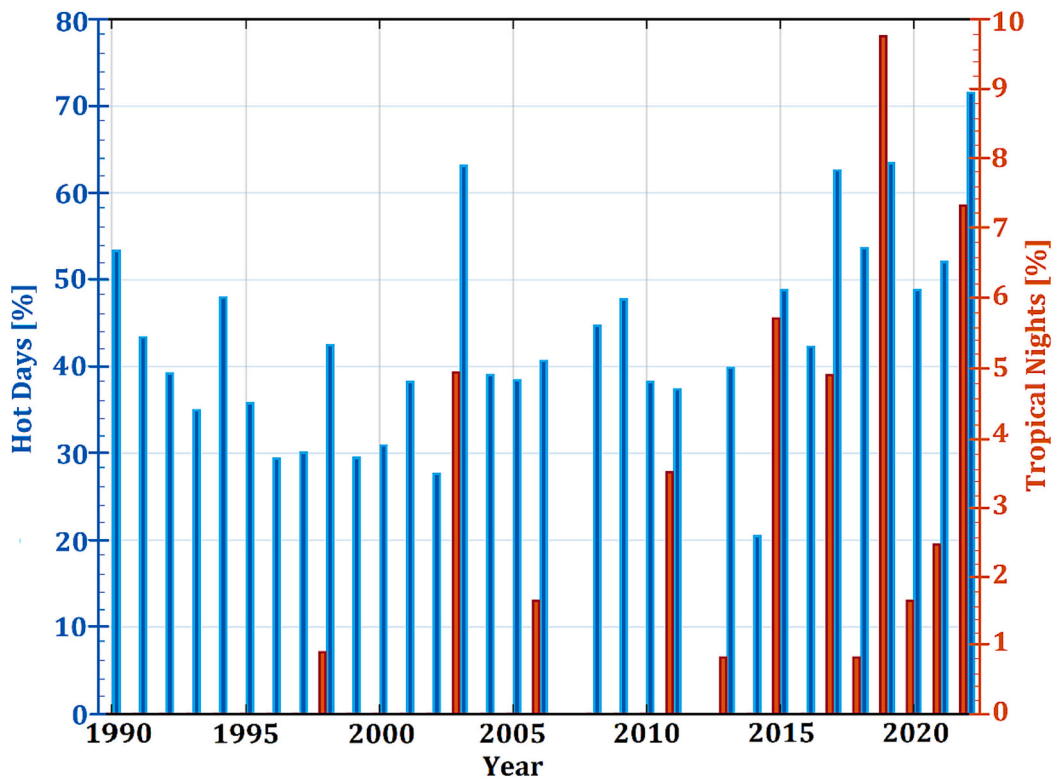


Fig. 4. Number of hot days, tropical nights and combined hot and tropical, expressed as percentages of the total amount of data.

highest values during 2003 (63.1%), 2017 (62.6%), 2019 (63.4%), and 2022 (71.5%).

The percentages of CHTs and HDs are comparable, suggesting that all HDs are classified also as TNs, while not all TNs correspond to HDs. The highest number of CHTs occurs in 2019 (9.7%).

### 3.2. Analysis of daytime temperatures and MOCI in the 2014–2022 timespan

This Section provides an analysis of temperature and MOCI data in the 2014–2022 timespan, for daytime data only (i.e., from 8:00 to 22:00 CET).

#### 3.2.1. Daytime temperatures

Fig. 5 shows the daytime temperature anomalies of the May–August 2022 season compared to the 2014–2022 period. In addition, minimum, average and maximum monthly temperatures are listed in Tables 1S–5S, (Supplementary material). The year 2022 presents a positive anomaly such as 2015, 2017, 2018, 2019 and presents the highest value (equal to 2.1 °C) corresponding to about 4 times those of 2015 and 2019. The 2022 summer season is the hottest of the period under investigation, with the month of May contributing mainly thanks to an anomaly equal to 2.7 °C (Fig. 5). During June, the anomaly of 2022 is equal to 2.1 °C, lower only than that of 2019 (equal to 2.4 °C). The average temperatures of the years 2019 and 2022 are comparable (28.5 °C and 28.2 °C, respectively) and 2022 shows the highest minimum temperature (20.1 °C in 2022, 18.1 °C in 2019). The month of July also has the highest anomaly (about 2.5 °C) with respect to the other years. The month of August 2022 has a much lower anomaly (1.2 °C) than those of the other months. The years 2017–2020 have a positive anomaly (in August) together with 2022 which ranks third as the highest anomaly after 2019 (1.6 °C) and 2017 (1.4 °C). The minimum temperature is the highest together with that of 2019 (19.7 °C).

The yearly cumulative temperature is displayed in Fig. 6. This metric is similar to the cumulative heat defined by Perkins-Kirkpatrick and Lewis (2020) and listed in Section 2.4.2 but, unlike the cumulative heat, the cumulative temperature is calculated as the sum of the hourly temperatures during all days of the season and not just during the HW episodes.

#### 3.2.2. Daytime MOCI

Fig. 7 shows the percentage distribution of MOCI hourly data in the period 2014–2022. The years 2019 and 2022 experienced the worst thermal conditions, with about 30% of data falling into the discomfort range. However, the year 2022 shows a percentage of data in the cold range lower than the year 2019 (18% in 2022, 29% in 2019). Consequently, a higher percentage of data belongs to the comfort range (53% in 2022, 41% in 2019). This is due to the higher minimum temperatures of 2022 with respect to 2019, moving part of the data from the cold to the comfort range. The difference between the percentages of 2019 and 2022 and those of the following



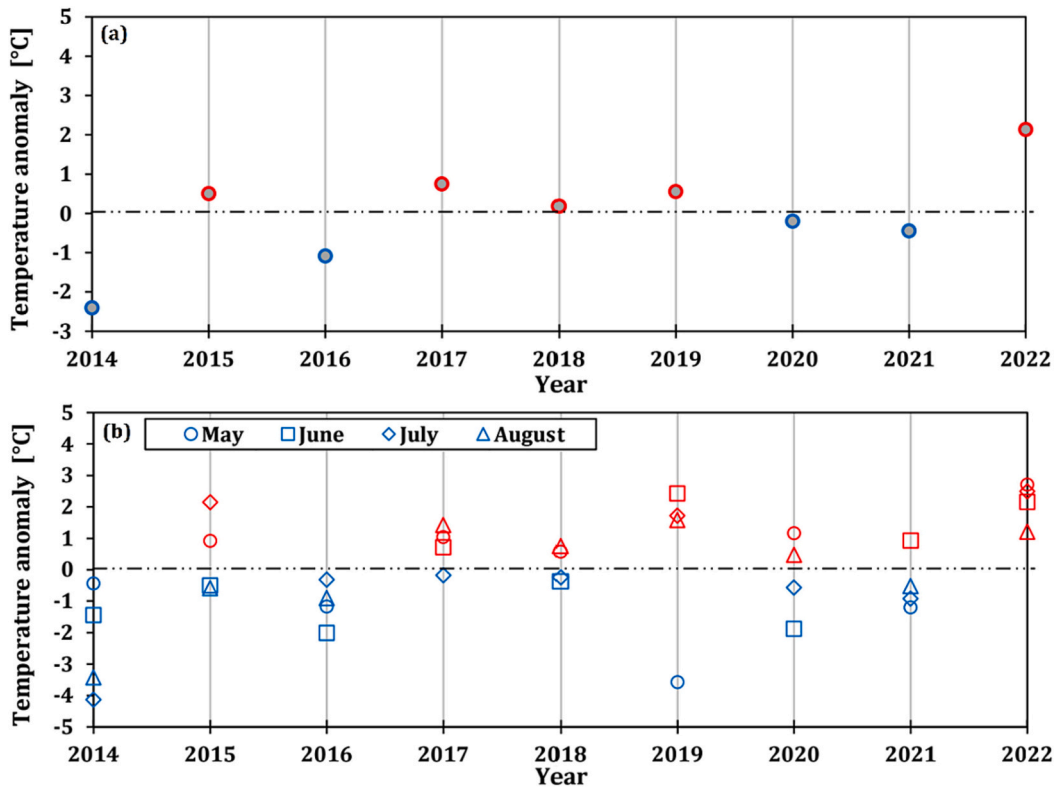


Fig. 5. Daytime temperature anomaly with respect to the control period 2014–2022 for: a) annual mean, b) monthly mean. Blue denotes negative anomalies and red denotes positive anomalies.

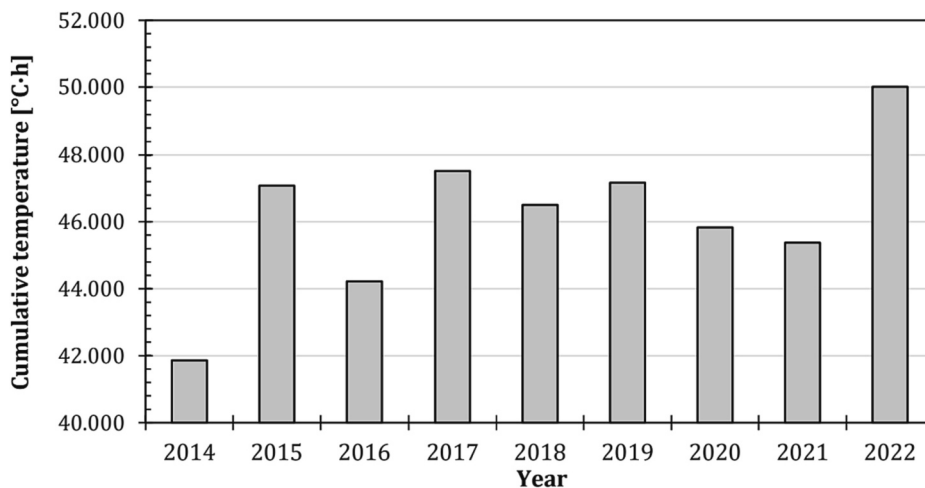


Fig. 6. Cumulative temperature across the May–August period for each year.

years is significant in the ranking of the percentages of data in the thermal stress range, i.e., the years of 2017 (22.88%) and 2015 (20.88%). The remaining years reveal thermal stress percentages equal to <20%. The lowest thermal stress portion, equal to about 6%, corresponds to 2014, which also shows the highest percentage of data in the cold range (50%). Consistent with what has been observed on temperatures, it is the coldest year.

Similarly to temperature, the cumulative daytime MOCI is calculated as the sum of the hourly MOCI values during the May–August season (Fig. 8).

The year of 2022 (with high minimum daytime temperatures) exhibits a cumulative temperature of 50,000 °C·h (47,000 °C·h in 2017, 2019 and 2015) and, unique among the years under investigation, has a cumulative MOCI higher than zero.

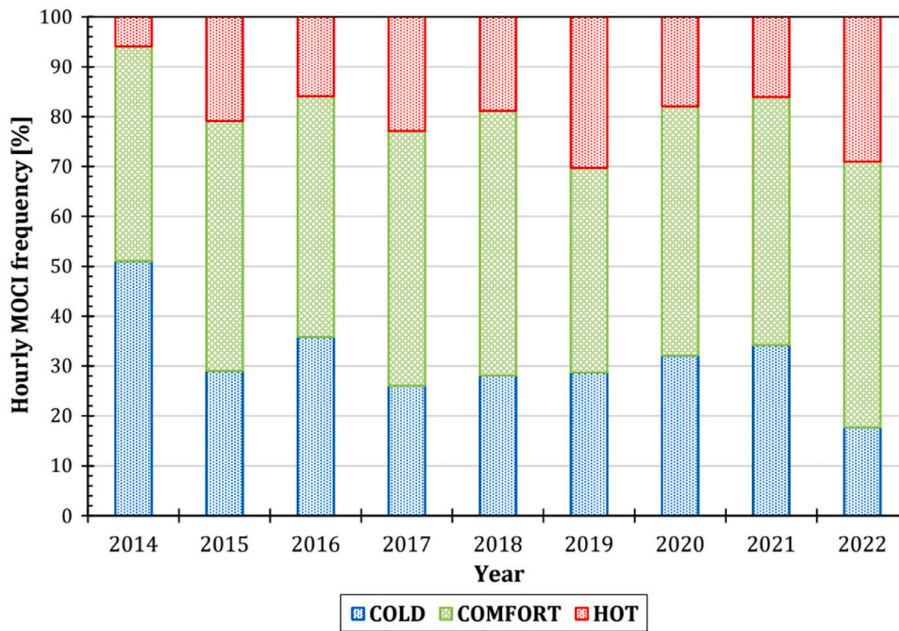


Fig. 7. Frequency plot. Percentages of hourly daytime MOCI corresponding to thermal sensations of cold (blue), comfort (green), and hot (red). (For interpretation of the references to colour in this figure legend, the reader is referred to the web version of this article.)

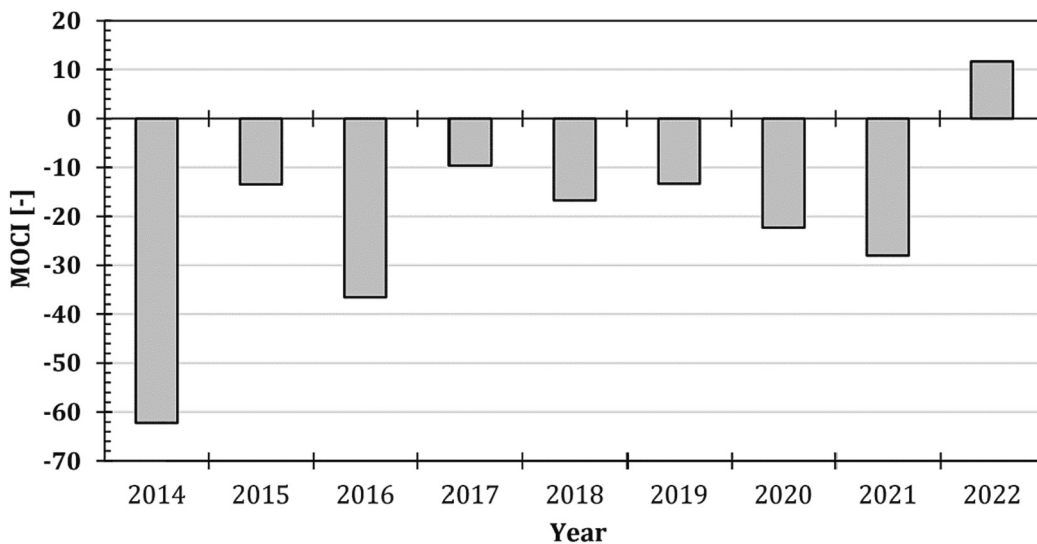


Fig. 8. Cumulative daytime MOCI across the May–August period for each year.

### 3.3. Thermo-hygrometric stress episodes

In this Section, the thermo-hygrometric stress episodes that occurred during the period 2014–2022 are analyzed. To this end, a range of metrics are derived from the climate change literature, as described in Section 2.4.

Fig. 9 displays the frequency (Fig. 9a) and the duration (Fig. 9b) of severe MOCI events, while Fig. 10 shows the cumulative extra-MOCI for severe thermo-hygrometric events. Table 4 lists the intensity of the thermo-hygrometric stress events for each year.

The years 2022, 2019, and 2017 have the highest occurrence of days meeting the definition of severe event (about 60), while during the other years the number remains under 50. The years 2019 (30 days) and 2022 (32 days) also have the highest duration of thermo-hygrometric stress episodes. The average MOCI during these events is equal to the comfort threshold in 2019 (0.5) and close to it in 2022, 2020, 2015 (0.4), while in the other years it is lower. The cumulative extra-MOCI is very high in 2019 (35.6) and slightly lower in 2022 (33.2), while the other years have accumulated extra-MOCI lower than 25.

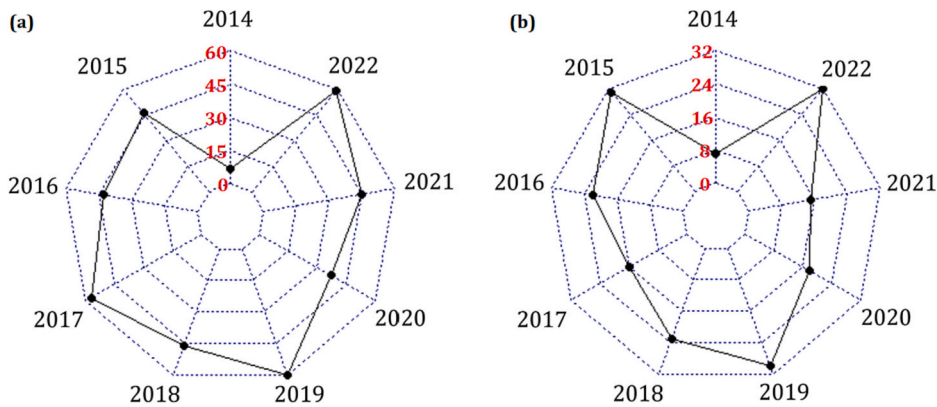


Fig. 9. (a) Severe MOCI events frequency, (b) Severe MOCI events duration.

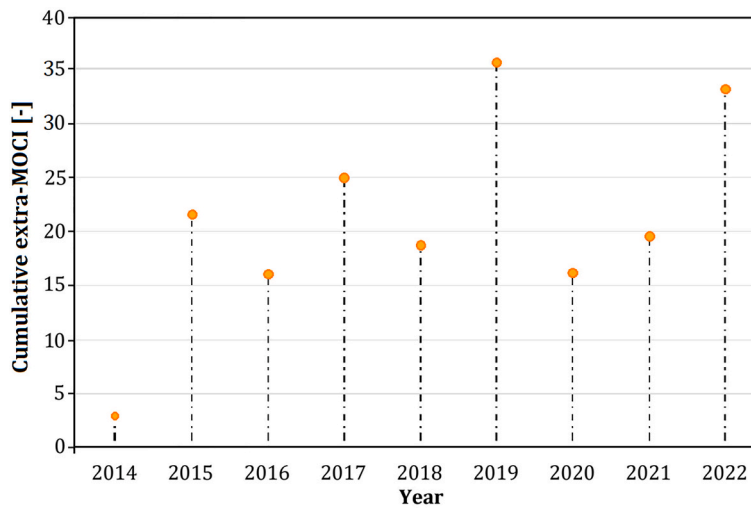


Fig. 10. Cumulative extra-MOCI for severe thermo-hygrometric events.

**Table 4**  
Thermo-hygrometric stress events intensity.

| Year | Thermo-hygrometric stress events intensity [-] |
|------|--|
| 2014 | 0.3  |
| 2015 | 0.4  |
| 2016 | 0.2  |
| 2017 | 0.3  |
| 2018 | 0.3  |
| 2019 | 0.5  |
| 2020 | 0.4  |
| 2021 | 0.3  |
| 2022 | 0.4  |

#### 4. Discussion

On average, the 1st May-31st August 2022 period in Milan results to be the hottest in the thirty-year 1991–2020 slot (temperature anomaly of 3.17 °C), with always positive anomalies compared to the monthly averages, among the highest in May, June and July and the lowest in August. The analysis of minimum and maximum temperatures reveals that the high positive anomaly of 2022 is essentially due to significantly higher minimum temperatures compared to the reference period and maximum temperatures in line with those of the control period. In particular, minimum temperatures fell below 21 °C in <30% of the nights of 2022. Since the minimum temperatures usually are measured at night, this confirms that the summer season of 2022 was particularly critical especially

for what concerns the minimum temperatures. These peculiarities of 2022 make it particularly suitable for this study as they allow to underline: i) the crucial effect of high minimum temperatures on people's thermo-hygrometric comfort, ii) the importance of studying severe thermo-hygrometric discomfort in addition to thermal ones, such as heat waves. As pointed out by Fischer and Schär (2010), high minimum temperatures have important repercussions on people's health since they "strongly amplify health effects by inhibiting the recovery from the daytime heat and by exacerbating the impact through sleep deprivation".

The analysis of the daytime (08–22 CET) MOCI is focused on the period where all the weather variables involved are available (i.e., 2014–2022) and a parallel analysis of temperatures in the same period and time slot is carried out as a comparison. The years 2022, 2019 and 2017 are characterized by the highest values of metrics describing the severe MOCI events (e.g., frequency, cumulative extra-MOCI). The fact that these years present the highest maximum and average temperatures in the control period confirms the key role of extreme temperatures in thermal stress events. However, it is crucial to evaluate also the overall thermal and thermo-hygrometric loads that the human body undergoes during the warm season. In this sense, the cumulative temperature and MOCI introduced here are explanatory. Cumulative temperature and MOCI allow for quantifying the thermal and thermo-hygrometric load the human body has been subjected to, regardless of the occurrence of HWs. The year 2022 presents the highest cumulative temperature, equal to about 50,000 °C•h, quite greater than those of 2017, 2019 and 2015 (around 47,000 °C•h). Starting from 2014, all years have negative cumulative MOCI apart from 2022 (value of about 175), with the years of 2017, 2019, and 2015 experiencing the lowest absolute values. It is important to underline that the years 2019 and 2022 present the same fraction of data in the thermal discomfort range (Fig. 7). Furthermore, the years 2019, 2017 and 2015 present a cold segment higher than 2022. This suggests that the minimum daytime temperatures significantly affect the "thermo-hygrometric load". This point is crucial in the evaluation of the thermo-hygrometric conditions as it regulates the existence of restoration for people.

Thermo-hygrometric stress events must necessarily be defined including the multiplicity of environmental and individual factors affecting human thermal sensations, as described in the Introduction. Many indices have been proposed to express the outdoor thermo-hygrometric sensations for a normotype through a defined and quantifiable numerical quantity (Coccolo et al., 2016). However, the adaptation of people to the climatic conditions they usually live in, makes it preferable to use a specifically conceived measure for the geographic region considered and the resident population, such as MOCI for the Mediterranean region. The year 2022 has one of the highest number of days falling in severe MOCI events (about 60 days) and one of the highest durations of thermo-hygrometric stress episodes (32 days), with an average value of MOCI quite close to the comfort threshold (0.5) during these events. Furthermore, the cumulative extra-MOCI is very high in 2022 (33.2), slightly lower only than in 2019 (35.6).

Although the results presented in this article present a regional connotation as they are based on the case study of the city of Milan, the methodology proposed can be easily generalized as based on common indices that can be applied in any geographical region with proper adaptations. For example, the MOCI index can be replaced with the index appropriate for the selected geographical region or with a universal index.

## 5. Conclusions

Similarly to extreme temperature events such as heat waves, extreme events of thermo-hygrometric discomfort also need to be identified and monitored to protect the health of populations, especially the most vulnerable groups. As discussed in the Introduction, the current literature lacks suitable indices for this. The purpose of this study is thus the proposal of a tool for the identification and characterization of thermo-hygrometric stress episodes, arranging indices derived from climate sciences. Such indices originally refer to HWs and consider the air temperature as reference quantity. Otherwise, in this paper, MOCI is treated as the reference quantity, due to its proven effectiveness in quantifying people's thermal sensations. Compared to the analogous apparatus for HWs, the bioclimatic index MOCI accounts for further parameters in addition to the temperature, namely weather quantities (relative humidity, wind speed and solar radiation) and personal conditions (i.e., the clothing) that significantly affect human thermal sensations. Thanks to the definition of a thermo-hygrometric stress event, based on a MOCI threshold equal to 0.5, this tool provides metrics describing frequency, intensity, and duration of severe episodes. Cumulative temperature and cumulative MOCI are introduced to describe the thermo-hygrometric load affecting the human body. To verify the validity of such a framework, it is applied to one of the hottest summers of the last decades, namely the May–August season of the year 2022, in the city of Milan (Po Valley, Italy).

The presented method has proved to be useful and effective in the identification of thermo-hygrometric stress events. Furthermore, it goes beyond the main limit of an approach based only on extreme meteorological and biometeorological states lying on information about no-stress thermal conditions, which represent important opportunities for the human body restoration. If such conditions are short or even worse, absent, the human body cannot recover, with consequent amplification of thermal stress sensations. On the other hand, although this work focuses on the urban environment, afflicted by the typical local overheating (i.e., the UHI) and the large number of people involved, it proposes a methodology extendable to non-urban environments without any adjustment or limitation.

## CRedit authorship contribution statement

**Serena Falasca:** Conceptualization, Methodology, Software, Formal analysis, Investigation, Resources, Data curation, Writing – original draft, Writing – review & editing. **Annalisa Di Bernardino:** Conceptualization, Methodology, Writing – review & editing, Visualization. **Ferdinando Salata:** Conceptualization, Methodology, Writing – review & editing, Visualization, Supervision.

## Declaration of Competing Interest

The authors declare that they have no known competing financial interests or personal relationships that could have appeared to influence the work reported in this paper.

## Data availability

The data are available free of charge on the ARPA Lombardia web page

## Acknowledgements

Serena Falasca was funded by MUR (Ministero dell'Università e della Ricerca of Italy) under PON "Ricerca e Innovazione" 2014-2020 (D.M. 1062/2021). The authors gratefully acknowledge ARPA Lombardia for providing weather data.

## Appendix A. Supplementary data

Supplementary data to this article can be found online at <https://doi.org/10.1016/j.uclim.2023.101728>.

## References

- Almazroui, M., 2020. Rainfall trends and extremes in Saudi Arabia in recent decades. *Atmosphere* 11, 964. <https://doi.org/10.3390/atmos11090964>.
- Bajšanski, I.V., Milošević, D.D., Savić, S.M., 2015. Evaluation and improvement of outdoor thermal comfort in urban areas on extreme temperature days: applications of automatic algorithms. *Build. Environ.* 94, 632–643. <https://doi.org/10.1016/j.buildenv.2015.10.019>.
- Balogun, I.A., Daramola, M.T., 2019. The outdoor thermal comfort assessment of different urban configurations within Akure City, Nigeria. *Urban Clim.* 29, 100489. <https://doi.org/10.1016/j.uclim.2019.100489>.
- Beck, H.E., Zimmermann, N.E., McVicar, T.R., Vergopolan, N., Berg, A., Wood, E.F., 2018. Present and future Köppen-Geiger climate classification maps at 1-km resolution. *Sci. Data* 5, 180214. <https://doi.org/10.1038/sdata.2018.214>.
- Caserini, S., Giani, P., Cacciamani, C., Ozgen, S., Lonati, G., 2017. Influence of climate change on the frequency of daytime temperature inversions and stagnation events in the Po Valley: historical trend and future projections. *Atmos. Res.* 184, 15–23. <https://doi.org/10.1016/j.atmosres.2016.09.018>.
- Chen, R., Lu, R., 2014. Dry tropical nights and wet extreme heat in Beijing: atypical configurations between high temperature and humidity. *Mon. Weather Rev.* 142, 1792–1802. <https://doi.org/10.1175/MWR-D-13-00289.1>.
- Coccolo, S., Kämpf, J., Scartezzini, J.-L., Pearlmutter, D., 2016. Outdoor human comfort and thermal stress: a comprehensive review on models and standards. *Urban Clim.* 18, 33–57.
- Cramer, W., Guiot, J., Fader, M., Garrabou, J., Gattuso, J.-P., Iglesias, A., Lange, M.A., Lionello, P., Llasat, M.C., Paz, S., Peñuelas, J., Snoussi, M., Toreti, A., Tsimplis, M.N., Xoplaki, E., 2018. Climate change and interconnected risks to sustainable development in the Mediterranean. *Nat. Clim. Chang.* 8, 972–980. <https://doi.org/10.1038/s41558-018-0299-2>.
- Di Bernardino, A., Iannarelli, A.M., Diémoz, H., Casadio, S., Cacciani, M., Siani, A.M., 2022. Analysis of two-decade meteorological and air quality trends in Rome (Italy). *Theor. Appl. Climatol.* 149, 291–307. <https://doi.org/10.1007/s00704-022-04047-y>.
- ETCCDI, 2020. Climate Change Indices - Definitions of the 27 Core Indices [WWW Document]. [http://etccdi.pacificclimate.org/list\\_27\\_indices.shtml](http://etccdi.pacificclimate.org/list_27_indices.shtml).
- Falasca, S., Ciancio, V., Salata, F., Golasi, I., Rosso, F., Curci, G., 2019. High albedo materials to counteract heat waves in cities: an assessment of meteorology, buildings energy needs and pedestrian thermal comfort. *Build. Environ.* 163, 106242. <https://doi.org/10.1016/j.buildenv.2019.106242>.
- Falasca, S., Curci, G., Salata, F., 2021. On the association between high outdoor thermo-hygrometric comfort index and severe ground-level ozone: a first investigation. *Environ. Res.* 195, 110306. <https://doi.org/10.1016/j.envres.2020.110306>.
- Falasca, S., Di Bernardino, A., Ciancio, V., Curci, G., Salata, F., 2022. A preliminary study of summer thermo-hygrometric comfort under different environmental conditions in a Mediterranean City. *Urban Sci.* 6, 51. <https://doi.org/10.3390/urbansci6030051>.
- Fanta, S.S., Yesuf, M.B., Saeed, S., Bhattacharjee, S., Hossain, Md.S., 2022. Analysis of precipitation and temperature trends under the impact of climate change over ten districts of Jimma Zone, Ethiopia. *Earth Syst. Environ.* <https://doi.org/10.1007/s41748-022-00322-0>.
- Ferrero, L., Riccio, A., Ferrini, B.S., D'Angelo, L., Rovelli, G., Casati, M., Angelini, F., Barnaba, F., Gobbi, G.P., Cataldi, M., Bolzacchini, E., 2019. Satellite AOD conversion into ground PM10, PM2.5 and PM1 over the Po valley (Milan, Italy) exploiting information on aerosol vertical profiles, chemistry, hygroscopicity and meteorology. *Atmos. Pollut. Res.* 10, 1895–1912. <https://doi.org/10.1016/j.apr.2019.08.003>.
- Fischer, E.M., Schär, C., 2010. Consistent geographical patterns of changes in high-impact European heatwaves. *Nat. Geosci.* 3, 398–403. <https://doi.org/10.1038/ngeo866>.
- García-Herrera, R., Díaz, J., Trigo, R.M., Luterbacher, J., Fischer, E.M., 2010. A review of the European summer heat wave of 2003. *Crit. Rev. Environ. Sci. Technol.* 40, 267–306. <https://doi.org/10.1080/10643380802238137>.
- Golasi, I., Salata, F., de Lieto Vollaro, E., Coppi, M., de Lieto Vollaro, A., 2016. Thermal perception in the Mediterranean area: comparing the Mediterranean outdoor comfort index (MOCI) to other outdoor thermal comfort indices. *Energies* 9, 550. <https://doi.org/10.3390/en9070550>.
- Graczyk, D., Pińskwar, I., Kundzewicz, Z.W., Hov, Ø., Førland, E.J., Szwed, M., Choryński, A., 2017. The heat goes on—changes in indices of hot extremes in Poland. *Theor. Appl. Climatol.* 129, 459–471. <https://doi.org/10.1007/s00704-016-1786-x>.
- ISTAT, 2022. <https://www.comune.milano.it/aree-tematiche/dati-statistici/pubblicazioni/popolazione-residente-a-milano> (last accessed on 28 September 2022).
- Khan, A., Papazoglou, E.G., Cartalis, C., Philippopoulos, K., Vasilakopoulou, K., Santamouris, M., 2022. On the mitigation potential and urban climate impact of increased green infrastructures in a coastal mediterranean city. *Build. Environ.* 221, 109264. <https://doi.org/10.1016/j.buildenv.2022.109264>.
- Khomsi, K., Chelhaoui, Y., Alilou, S., Souiri, R., Najmi, H., Souhaili, Z., 2022. Concurrent heat waves and extreme ozone (O3) episodes: combined atmospheric patterns and impact on human health. *IJERPH* 19, 2770. <https://doi.org/10.3390/ijerph19052770>.
- King, A.D., Karoly, D.J., 2017. Climate extremes in Europe at 1.5 and 2 degrees of global warming. *Environ. Res. Lett.* 12, 114031. <https://doi.org/10.1088/1748-9326/aa8e2c>.
- Kovats, R.S., Kristie, L.E., 2006. Heatwaves and public health in Europe. *Eur. J. Pub. Health* 16, 592–599. <https://doi.org/10.1093/eurpub/ckl049>.
- Lai, D., Liu, W., Gan, T., Liu, K., Chen, Q., 2019. A review of mitigating strategies to improve the thermal environment and thermal comfort in urban outdoor spaces. *Sci. Total Environ.* 661, 337–353. <https://doi.org/10.1016/j.scitotenv.2019.01.062>.
- Lavaysse, C., Cammalleri, C., Dosio, A., van der Schrier, G., Toreti, A., Vogt, J., 2018. Towards a monitoring system of temperature extremes in Europe. *Nat. Hazards Earth Syst. Sci.* 18, 91–104. <https://doi.org/10.5194/nhess-18-91-2018>.

- Li, X., Zhou, Y., Yu, S., Jia, G., Li, H., Li, W., 2019. Urban heat island impacts on building energy consumption: a review of approaches and findings. *Energy* 174, 407–419. <https://doi.org/10.1016/j.energy.2019.02.183>.
- Linares, C., Díaz, J., Negev, M., Martínez, G.S., Debono, R., Paz, S., 2020. Impacts of climate change on the public health of the Mediterranean basin population - current situation, projections, preparedness and adaptation. *Environ. Res.* 182, 109107 <https://doi.org/10.1016/j.envres.2019.109107>.
- Lionello, P., Scarascia, L., 2018. The relation between climate change in the Mediterranean region and global warming. *Reg. Environ. Chang.* 18, 1481–1493. <https://doi.org/10.1007/s10113-018-1290-1>.
- Lomakina, N.Ya., Lavrinenko, A.V., 2022. Modern trends of temperature of the atmospheric boundary layer over Siberia. *Atmos. Ocean. Opt.* 35, 378–386. <https://doi.org/10.1134/S102485602204011X>.
- Mbokodo, I., Bopape, M.-J., Chikoore, H., Engelbrecht, F., Nethengwe, N., 2020. Heatwaves in the future warmer climate of South Africa. *Atmosphere* 11, 712. <https://doi.org/10.3390/atmos11070712>.
- NOAA, January 2022. National Centers for Environmental Information, State of the Climate: Monthly Global Climate Report for Annual 2021. published online. retrieved on September 19, 2022 from. <https://www.ncei.noaa.gov/access/monitoring/monthly-report/global/202113>.
- Perkins, S.E., Alexander, L.V., 2013a. On the measurement of heat waves. *J. Clim.* 26, 4500–4517. <https://doi.org/10.1175/JCLI-D-12-00383.1>.
- Perkins, S.E., Alexander, L.V., 2013b. On the measurement of heat waves. *J. Clim.* 26, 4500–4517. <https://doi.org/10.1175/JCLI-D-12-00383.1>.
- Perkins-Kirkpatrick, S.E., Gibson, P.B., 2017. Changes in regional heatwave characteristics as a function of increasing global temperature. *Sci. Rep.* 7, 12256. <https://doi.org/10.1038/s41598-017-12520-2>.
- Perkins-Kirkpatrick, S.E., Lewis, S.C., 2020. Increasing trends in regional heatwaves. *Nat. Commun.* 11, 3357. <https://doi.org/10.1038/s41467-020-16970-7>.
- Putaud, J.-P., Van Dingenen, R., Alastuey, A., Bauer, H., Birmili, W., Cyrys, J., Flentje, H., Fuzzi, S., Gehrig, R., Hansson, H.C., Harrison, R.M., Herrmann, H., Hitenberger, R., Hüglin, C., Jones, A.M., Kasper-Giebl, A., Kiss, G., Kousa, A., Kuhlbusch, T.A.J., Löschan, G., Maenhaut, W., Molnar, A., Moreno, T., Pekkanen, J., Perrino, C., Pitz, M., Puxbaum, H., Querol, X., Rodriguez, S., Salma, I., Schwarz, J., Smolik, J., Schneider, J., Spindler, G., ten Brink, H., Tursic, J., Viana, M., Wiedensohler, A., Raes, F., 2010. A European aerosol phenomenology – 3: physical and chemical characteristics of particulate matter from 60 rural, urban, and kerbside sites across Europe. *Atmos. Environ.* 44, 1308–1320. <https://doi.org/10.1016/j.atmosenv.2009.12.011>.
- Rozbicka, K., Rozbicki, T., 2021. Long-term variability of bioclimatic conditions and tourism potential for Warsaw agglomeration (Poland). *Int. J. Biometeorol.* 65, 1485–1495. <https://doi.org/10.1007/s00484-020-01957-2>.
- Russo, S., Sterl, A., 2011. Global changes in indices describing moderate temperature extremes from the daily output of a climate model. *J. Geophys. Res.* 116, D03104. <https://doi.org/10.1029/2010JD014727>.
- Salata, F., Golasi, I., de Lieto Vollaro, R., de Lieto Vollaro, A., 2016. Outdoor thermal comfort in the Mediterranean area. A transversal study in Rome, Italy. *Build. Environ.* 96, 46–61. <https://doi.org/10.1016/j.buildenv.2015.11.023>.
- Scorzini, A.R., Leopardi, M., 2019. Precipitation and temperature trends over Central Italy (Abruzzo region): 1951–2012. *Theor. Appl. Climatol.* 135, 959–977. <https://doi.org/10.1007/s00704-018-2427-3>.
- Shin, J.-Y., Kang, M., Kim, K.R., 2022. Outdoor thermal stress changes in South Korea: increasing inter-annual variability induced by different trends of heat and cold stresses. *Sci. Total Environ.* 805, 150132 <https://doi.org/10.1016/j.scitotenv.2021.150132>.
- Shooshtarian, S., Lam, C.K.C., Kenawy, I., 2020. Outdoor thermal comfort assessment: a review on thermal comfort research in Australia. *Build. Environ.* 177, 106917 <https://doi.org/10.1016/j.buildenv.2020.106917>.
- Tang, K.H.D., 2019. Climate change in Malaysia: trends, contributors, impacts, mitigation and adaptations. *Sci. Total Environ.* 650, 1858–1871. <https://doi.org/10.1016/j.scitotenv.2018.09.316>.
- Tomczyk, A.M., Bednorz, E., Matzarakis, A., 2020. Human-biometeorological conditions during heat waves in Poland. *Int. J. Climatol.* 40, 5043–5055. <https://doi.org/10.1002/joc.6503>.
- Unger, J., Skarbit, N., Kovács, A., Gál, T., 2020. Comparison of regional and urban outdoor thermal stress conditions in heatwave and normal summer periods: a case study. *Urban Clim.* 32, 100619 <https://doi.org/10.1016/j.uclim.2020.100619>.
- Varentsov, M., Shartova, N., Grischenko, M., Konstantinov, P., 2020. Spatial patterns of human thermal comfort conditions in Russia: present climate and trends. *Weather Clim. Soc.* 12, 629–642. <https://doi.org/10.1175/WCAS-D-19-0138.1>.
- Viceto, C., Cardoso Pereira, S., Rocha, A., 2019. Climate change projections of extreme temperatures for the Iberian Peninsula. *Atmosphere* 10, 229. <https://doi.org/10.3390/atmos10050229>.
- Wang, P., Yang, Y., Ji, C., Huang, L., 2023. Positivity and difference of influence of built environment around urban park on building energy consumption. *Sustain. Cities Soc.* 89, 104321 <https://doi.org/10.1016/j.scs.2022.104321>.
- World Meteorological Organization (WMO), 2022. Available online: <https://public.wmo.int/en/media/press-release/wmo-update-5050-chance-of-global-temperature-temporarily-reaching-15%C2%B0c-threshold> (accessed on 21st September 2022).
- Zeng, D., Wu, J., Mu, Y., Deng, M., Wei, Y., Sun, W., 2020. Spatial-temporal pattern changes of UTCI in the China-Pakistan economic corridor in recent 40 years. *Atmosphere* 11, 858. <https://doi.org/10.3390/atmos11080858>.
- Zittis, G., Hadjinicolaou, P., Fnais, M., Lelieveld, J., 2016. Projected changes in heat wave characteristics in the eastern Mediterranean and the Middle East. *Reg. Environ. Chang.* 16, 1863–1876. <https://doi.org/10.1007/s10113-014-0753-2>.